International Journal of Legal Medicine (2018) 132:939–954
https://doi.org/10.1007/s00414-017-1764-6

ORIGINAL ARTICLE

Revisited larval morphology of Thanatophilus rugosus (Coleoptera: Silphidae)

Martin Novák[1] · Pavel Jakubec[1] · Jarin Qubaiová[1] · Hana Šuláková[1,2] · Jan Růžička[1]

Received: 27 September 2017 / Accepted: 12 December 2017 / Published online: 21 December 2017

Abstract

Determination of insect species and their instars, occurring on human remains, is important information that allows us to use insects for estimation of postmortem interval and detect possible manipulation with the body. However, larvae of many common species can be identified only by molecular methods, which is not always possible. The instar determination is even more challenging, and qualitative characters that would allow a more precise identification are mostly unknown. *Thanatophilus rugosus* (Linnaeus, 1758) is a common necrophagous beetle in the whole Palaearctic region from Europe to Japan. The species is often encountered on corpses of large vertebrates including humans, and its potential to become a useful bioindicator for forensic entomology is therefore high. Adults can be easily distinguished from other species; however, larvae were never thoroughly described to allow species and instar identification. The aim of this study was to provide reliable morphological characters that would allow species and instar identification of *T. rugosus* larvae. The material for morphological study was obtained from rearing under controlled conditions (20 °C and 12:12 h of light/dark period), and specimens that were not studied morphologically were allowed to complete their development. Quantitative and qualitative morphological characters for instar and species identification are described and illustrated. Additionally, we report observations of biology and developmental length for all stages of the species.

Keywords *Thanatophilus rugosus* · Larval instar identification · Morphology · Forensic entomology

Introduction

Beetles (Coleoptera) are one of the most diverse groups of animals, which can be commonly encountered on vertebrate carcasses around the world [1]. Despite this well-known fact, their value for forensic entomology was not fully recognized until recently [2]. The tight association between food source (corpse) and beetles can provide a lot of information regarding toxicological profile of the deceased, possible postmortem body manipulation, and approximate time of death (postmortem interval (PMI)) itself [3–6]. The last one is an especially important feature for homicide investigations. If a body is discovered after more than 72 h, the state of the body itself cannot provide accurate data for such an estimate [7].

When estimating the PMI based on insect evidence, it is crucial to establish how old are the earliest stages that were developing on the body at the time of its discovery [8]. The most common way of how to calculate such an estimate is to use a thermal summation model [9]. These models are species- and stage-specific [5]; hence, to give an accurate estimate of PMI, the species and development stage have to be identified correctly. However, the identification of larval instars or even beetle species can be challenging.

Amendt et al. [10] offer two approaches that can be used to resolve the issue of species identification. The first is to rear the eggs and larvae to adulthood. At that stage, the abundance of literature can be used for morphological identification. The disadvantage of this method is that the development takes time and the results are highly uncertain due to possible mortality

Electronic supplementary material The online version of this article (https://doi.org/10.1007/s00414-017-1764-6) contains supplementary material, which is available to authorized users.

✉ Pavel Jakubec
jakubecp@fzp.czu.cz

[1] Faculty of Environmental Sciences, Czech University of Life Sciences Prague, Kamýcká 129, Praha 6 –, 165 21 Suchdol, Czech Republic

[2] Police of the Czech Republic, Institute of Criminalistics Prague, P.O. Box 62/KUP, 170 89 Prague, Czech Republic

during rearing. The second approach recommended by the authors is to analyze specimens' DNA, which is currently a standard method in forensic investigations. Nevertheless, closely related or hybrid species can be difficult to distinguish, especially when the data on the level of their intraspecific and interspecific DNA variability are scarce [11, 12]. It is also worth mentioning that DNA extraction from old or badly preserved specimens could be difficult, expensive, or completely impossible [13, 14].

The second part of the problem is the issue of precise and accurate stage identification. A simple and elegant solution was provided by the discovery of Dyar's Rule, which states that the size of morphological characters between successive instars follows geometrical progression [15, 16]. This idea and its derivatives were used to create body size frequency distribution models and other models for identification of all larval instars of some forensically important species [17–21]. The simplicity of this approach, nonetheless, comes with a cost, because it is prone to errors when applied to animals from different geographical populations and breeding conditions other than the ones originally measured [22].

The solution to all of these problems could be a detailed morphological description of all developmental stages, which would reveal stage-specific qualitative characters and thus allow species and instar identification.

The genus *Thanatophilus* Leach, 1815, has currently 23 valid species: 14 are Palaearctic, four Nearctic, two Holarctic, and three Afrotropical in distribution [23–25]. The phylogenetic position of *Thanatophilus* is a sister branch to remaining Holarctic genera of Silphinae, together forming a cluster which is a sister group to Neotropical and Australian *Oxelytrum* Gistel, 1848, and *Ptomaphila* Kirby & Spence, 1828 [26, 27]. Taxonomy and classifications of *Thanatophilus* species based on adult morphology were reviewed by Schawaller [28], with later additions from Kozminykh [29], Růžička [30], and Ji [31]. The larvae of this genus are poorly known with only eight described species. These descriptions are often based on an unknown larval instar, and many of them are rather brief and without illustrations (see Table 1).

We choose *Thanatophilus rugosus* (Linnaeus, 1978) as our focal species because it is a widely distributed Palaearctic beetle, known to occur from Europe to Japan [25]. In Europe, it is considered a very common necrophagous beetle [41–43]. Similar to other carrion beetles (Silphidae) [5, 6, 44, 45], this species could also become a highly valuable forensic indicator as its presence was detected on 16% of the cases in the Czech Republic when the entomological evidence was collected (Šuláková, unpublished data) ($N = 23$ out of 144 cases between 2003 and 2016).

Little is known about the immature stages of *T. rugosus*. The first description of an unknown larval stage and some remarks about the biology of adults were published by Xambeu [38], but the description is not detailed enough to allow species identification. The second and last description of its larval morphology was done by Lengerken [33], and it depicts all three instars of *T. rugosus*. His portrayal was much more thorough than Xambeu's, although he himself admits that species identification of the larval stages of *T. rugosus*, *T. dispar*, and *T. sinuatus* requires comparative material and that the size-based instar identification, which he recognized as the only solution, is prone to errors due to the high morphological plasticity under different breeding conditions.

The aim of this paper is to provide a morphological description of all larval stages with special regard to characters and parts that were omitted in previous reports and to identify the characters that are species- and instar-specific. These characters would allow the identification of even badly preserved specimens when DNA analysis is difficult or does not answer the questions (e.g., to which instar the specimen belongs).

Table 1 List of species in genus *Thanatophilus* with described larvae. Only original morphological descriptions were included

Species	Author	Described stage	Comments
Thanatophilus capensis (Wiedemann, 1821)	Daniel et al. [32]	All three instars	Described and illustrated
Thanatophilus coloradensis (Wickham, 1902)	Anderson and Peck [23]	Probably 3rd instar	Described and partially illustrated
Thanatophilus dispar (Herbst, 1793)	von Lengerken [33, 34]	All three instars	Brief description and illustration
Thanatophilus lapponicus (Herbst, 1793)	Dorsey [35]	3rd instar	Described and illustrated
Thanatophilus micans (Fabricius, 1794)	Paulian [36]	Probably 3rd instar	Described and illustrated
Thanatophilus micans (Fabricius, 1794)	Prins [37]	Egg, three larval instars and pupa	Described and illustrated
Thanatophilus micans (Fabricius, 1794)	Daniel et al. [32]	All three instars	Described and illustrated
Thanatophilus rugosus (Linnaeus, 1758)	Xambeu [38]	Probably 3rd instar	Brief description
Thanatophilus rugosus (Linnaeus, 1758)	von Lengerken [33]	All three instars and pupa	Described and illustrated
Thanatophilus sinuatus (Fabricius, 1775)	Xambeu [39]	Probably 3rd instar	Brief description
Thanatophilus sinuatus (Fabricius, 1775)	von Lengerken [33 34]	All three instars and pupa	Described and illustrated
Thanatophilus sinuatus (Fabricius, 1775)	Paulian [36]	Probably 3rd instar	Brief description and illustration
Thanatophilus trituberculatus (Kirby, 1837)	Anderson [40]	Probably 3rd instar	Brief description and illustration

Material and methods

Adult specimens of *T. rugosus* were collected by baited pitfall traps around Albeř (Czech Republic) (49° 01′ 35.7″ N 15° 08′ 54.9″ E) between 16th and 20th May 2016. Subsequently, they were transferred to the laboratory, where they were kept in small breeding groups of five to eight individuals. These groups were placed inside well-ventilated plastic boxes (85 × 110 × 45 mm) with a 1-cm-thick layer of rough sand (diameter 1–4 mm) and were provided with fish meat (*Scomber scombrus* Linnaeus, 1758) ad libitum. Breeding and development of immature stages took place inside a climatic chamber with constant temperature of 20 °C and a 12-h light and 12-h darkness photoperiod regime, maintained by fluorescent light (Osram L 8 W/640).

Breeding boxes were thoroughly inspected at least once every 24 h, and the eggs were removed and separated and their development observed at the same frequency. Developmental milestones were recognized by the presence of exuvia. During each developmental stage (except pupa), we removed 6 to 10 specimens for morphological study and measurements. All selected specimens were killed in ethyl acetate fumes, fixed with hot water (90–95 °C), and stored in 75% alcohol solution. The rest was followed to record their development time, but only individuals with reliable known starting and finishing point are reported in Table 2. Due to this restriction, we had to exclude observations of several eggs, as the starting point of their development was unclear, because they were hidden among substrates (unlike majority of egg clutches that were found around the edges of breeding boxes).

Optical and electron imaging methodology follows Novák [46].

Optical imaging The fixed specimen were cleared by simple brush and then placed in Digital Ultrasonic Cleaner PS-06A. The detached heads were afterwards boiled in 10% potassium hydroxide (KOH) for clearer visibility of the delicate parts. Habitus was photographed while the specimen was submerged in ethanol; heads were photographed while being submerged in glycerol (due to better optical properties and higher stability thanks to higher viscosity of glycerol). Images were taken by a Canon macro photo lens MP-E 65 mm on a Canon 550D body, mounted on an automated macro rail for focus stacking (Cognisys StackShot). Smaller details were photographed using an Olympus BX53 microscope with an Olympus DP73 digital camera. The sets of pictures were consequently stacked into a final image with a high depth of field in Zerene Stacker 1.04 (64-bit) by Zerene Systems LLC.

Electron imaging For a detailed view of the morphology and body structure of the larvae, the samples were examined at the Faculty of Science of Charles University in Prague. The specimens were first dehydrated through a series of increasing alcohol concentrations. The samples were transferred sequentially to 60, 70, 80, 90, and 95% alcohol for ca. 0.5 h each. Dehydrated samples were then dried by a critical point drying method. Dry samples were subsequently attached to an aluminum disk target and coated with gold in Bal-Tec Sputter Coater SCD 050, to ensure conductivity. Electron imaging was performed using a JSM-6380LV (JEOL) scanning electron microscope (SEM) with a high resolution of 3.0 nm (30 kW).

Final figures from both optical and electron imaging were compiled using the GIMP ver. 2.8.16 graphic program; graphs were compiled using R ver. 3.4.1 statistical computing program.

Terminology and measurements Interpretation and terminology of larval and pupal descriptions follow Lawrence and Slipinski [47].The measurements were made by placing specimens under an Olympus SZX16 stereo microscope and measured with cellSens Entry 1.6 program. The following abbreviations are used in the text:

AI	length of antennomere I
AII	length of antennomere II
AIII	length of antennomere III
A1L	length of abdominal segment I
A1W	width of abdominal segment I
HL	head length (without labrum)
HW	head width (at the widest point)
LPI	length of labial palpomere I
LPII	length of labial palpomere II
MPI	length of maxillary palpomere I
MPII	length of maxillary palpomere II
MPIII	length of maxillary palpomere III
N1L	pronotal Length
N1W	pronotal width (at the widest point)
N2L	mesonotal length
N2W	mesonotal width (at the widest point)

Table 2 Development length of *Thanatophilus rugosus* at 20 °C and under a 12:12-h photoperiod

Stage	Egg	Instar I	Instar II	Instar III	Pupae
Mean length of development (in days)	3.397	3.061	5.583	19.777	13.659
Standard deviation (in days)	0.630	0.452	1.241	0.498	0.472
Number of observations	12	15	14	5	4

N3L	metanotal length
N3W	metanotal width (at the widest point)
URI	length of urogomphal segment I
URII	length of urogomphal segment II
URS	length of urogomphal terminal seta
N1L/W	ratio of pronotal length to pronotal width
N2L/W	ratio of mesonotal length to mesonotal width
N3L/W	ratio of metanotal length to metanotal width
HW/HL	ratio of head width to head length
A1L/W	ratio of abdominal segment I length to abdominal segment width

Results

Biology

We observed that breeding pairs did not reproduce in a photoperiod longer than 12:12 h (dark/light phases) such as 8:16 h. Females lay their eggs under the substrate in small clusters (usually around nine eggs per cluster) mainly along the edges and bottom of the breeding box. Before hatching, larvae are visible through the egg membrane, and shortly after hatching, they search for food in the proximity. They have a tendency to stay close to the food source most of the time.

In 20 °C, the development from egg to adult took on average more than 45 days. The mean length of development for each stage is given in Table 2. Species develops through three larval instars, and no variation was observed in this trait. Prolonged pupation and higher mortality were observed in individuals of the third instar if they are disturbed while preparing a pupation chamber. The disturbance was on our part motivated by the need for constant surveillance of the development progression. We solved the issue by limiting the available space for the chamber, which forced the larva to pupate next to the wall of the dish, so we could easily observe them without physically searching through the substrate.

Larvae often took the opportunity to cannibalize smaller or newly molted individuals, although the level of cannibalism was not very high as we limited the number of specimens in each dish and also provided the food ad libitum.

Morphometry

Online Resource 1 provides mean values of important morphological measurements and ratios for all three larval instars. We observed that some body parts of *T. rugosus* are not growing isometrically, but rather allometrically. This relationship is very prominent in the case of the size relationship between urogomphal segments I and II (Figs. 1a, b and 9c–e) and also between palpomeres I and II of labium (Figs. 1m–o and 2a, b). Figure 2a, b shows that one of the segments grows isometrically and the second one does not. This creates a proportional difference between their lengths and could be used as a character for instar identification.

The measurements of other body parts could also be used for instar identification. The full list is provided in Online

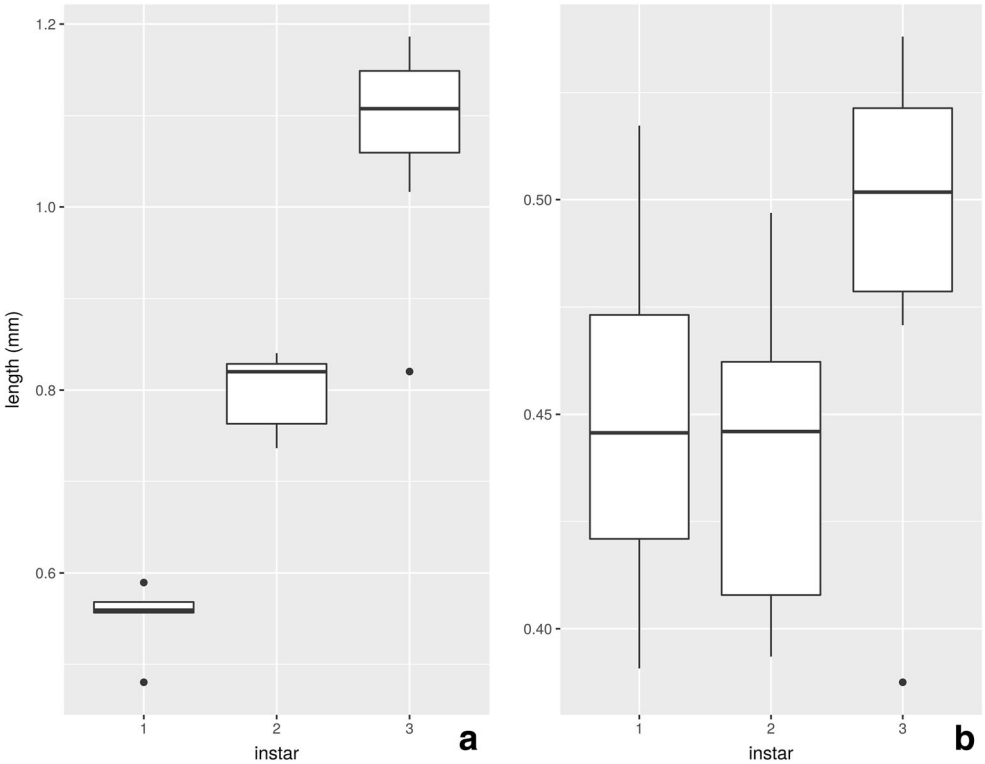

Fig. 1 Boxplots of length of urogomphal segments: segment I (**a**) and segment II (**b**) of all three larval instars of *Thanatophilus rugosus*. Horizontal lines within the boxes indicate median values; upper and lower boxes indicate the 75th and 25th percentiles, respectively; whiskers indicate the values with the 1.5 interquartile ranges; small, black dots are outliers

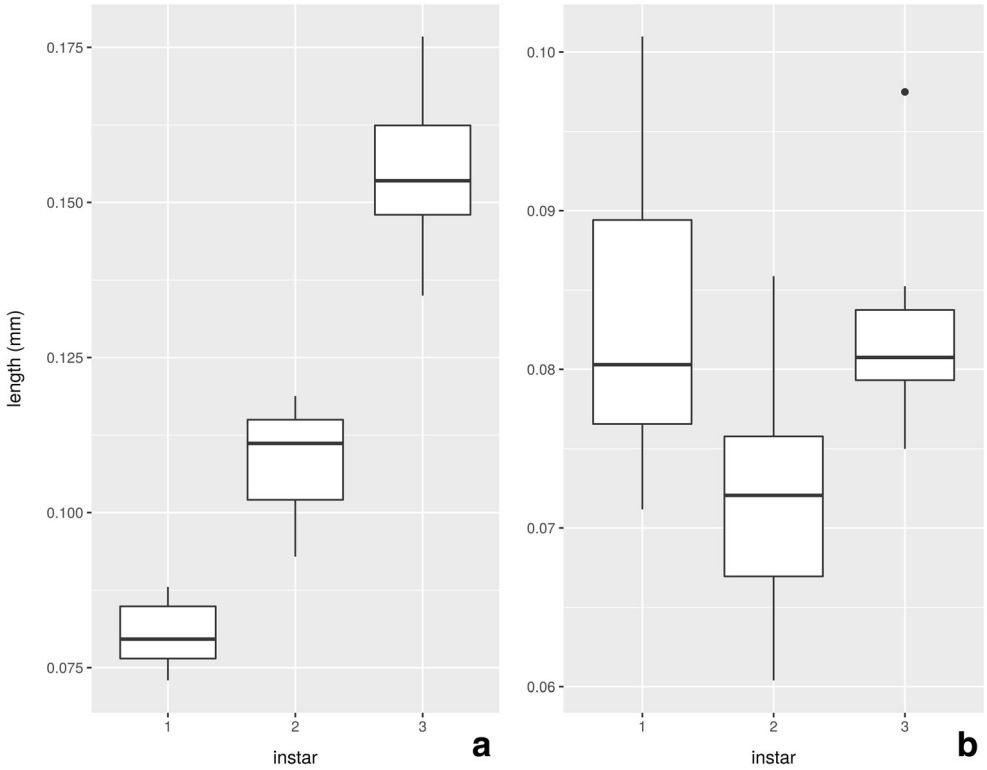

Fig. 2 Boxplots of length of labial palpomers: palpomere I (**a**) and palpomere II (**b**) of all three larval instars of *Thanatophilus rugosus*. Horizontal lines within the boxes indicate median values; upper and lower boxes indicate the 75th and 25th percentiles, respectively; whiskers indicate the values with the 1.5 interquartile ranges; small, black dots are outliers

Resource 1. The two measurements that are widely used for instar identification are head and pronotal width. We suggest to use head width (Fig. 3) for *T. rugosus* instar identification, as the supposed overlap among the instars was not observed in our dataset. For further comments on utilization of measurement-based characters, see the "Discussion" section.

Description of immature stages of *Thanatophilus rugosus*

Family SILPHIDAE Latreille, 1806
Sub-family Silphinae Latreille, 1806
Genus *Thanatophilus* Leach, 1815
Species *Thanatophilus rugosus* (Linnaeus, 1758)

Larvae

Body (Fig. 4 (a–i)): *Instar III* (Fig. 4 (a, d, g)). Mean value of total length: 13.25 ± 1.488 mm. Campodeiform larvae, more or less fusiform, widest at the metathorax and slightly narrowing towards both ends. Slender body only slightly dorsoventrally flattened. Head and all terga strongly sclerotized, and covered by vestiture of scattered setae. All terga on lateral margin with few long setae that can be clearly visible in dorsal or ventral view. Whole dorsal side with dark brown to black coloration. Abdominal paratergites small and pointed posteriorly with longest seta protruding in the direction of their apex. Ventral side of thorax white. Ventral area of segment I poorly sclerotized, white, with dark pigmentation only in the central area and far lateral edges. Segments II to VIII centrally dark with speckled dark lateral areas divided from the medial pigmentation by incomplete lighter stripe. Segment IX ventrally dark with lighter patches laterally. Segment X uniformly brown. Distal segments ventrally overall darker than proximal. *Instar II* (Fig. 4 (b, e, h)). Mean value of total length: 9.22 ± 1.45 mm. Ventral side of thorax white. Segment II ventrally sclerotized with two distinguishable white lines dividing central and lateral dark pigmented areas. Segments III to IX ventrally fully sclerotized and dark with slightly lighter central areas. *Instar I* (Fig. 4 (c, f, i)). Mean value of total length: 5.96 ± 0.898 mm. Ventral side of thorax white. Segment II ventrally sclerotized with two fine white lines dividing central and lateral dark pigmented areas. Segments III to IX ventrally fully sclerotized and dark.

Head capsule (Fig. 5a, d, e): *Instar III* (Figs. 4 (a, d, g) and 5e). Prognathous and protracted; HW 1.953 ± 0.15 mm, HL 1.144 ± 0.044 mm, HW/HL 1.711 ± 0.161; reniform in ventral view; gena short, about one fourth of the width of the head capsule in its longest width in dorsal view; head capsule dorsally covered with few long and many short stout setae. Epicranial stem present, frontal arms V-shaped, but with U-base as the angle changes in the middle of suture (Fig. 5a, d; *fa*), median endocarina absent. Six stemmata on each side of the head separated into two groups; four stemmata forming a trapezoid placed posteriorly behind antennal base, and two stemmata placed ventrally under antennal base, parallel to

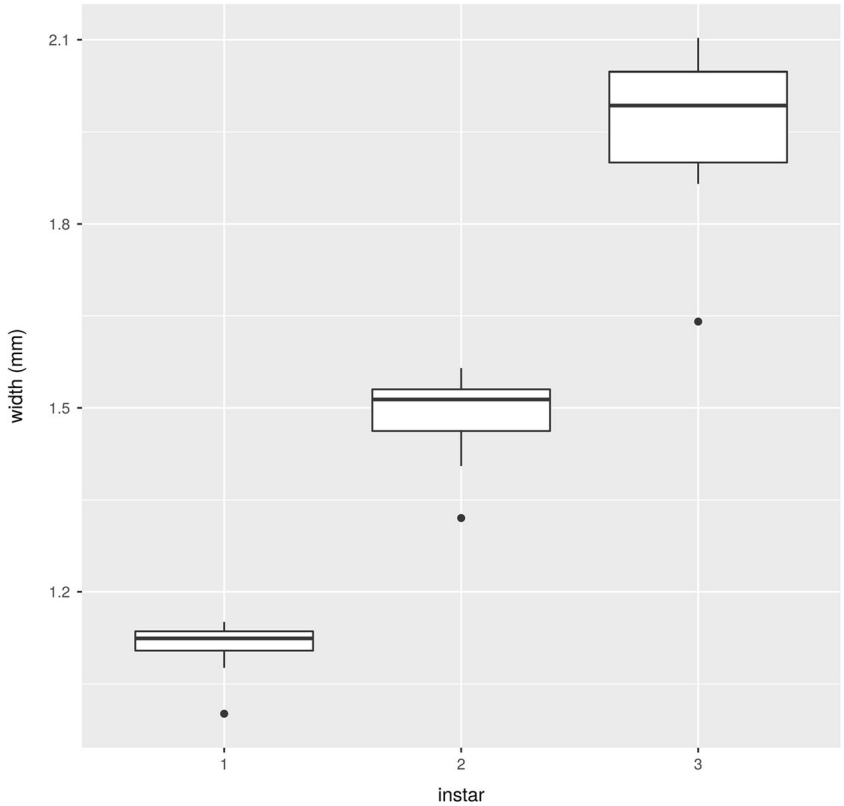

Fig. 3 Boxplots of head width of all larval instars of *Thanatophilus rugosus*. Horizontal lines within the boxes indicate median values; upper and lower boxes indicate the 75th and 25th percentiles, respectively; whiskers indicate the values with the 1.5 interquartile ranges; small, black dots are outliers

the wider base of the trapezoid (Fig. 6c). Frontoclypeal suture absent; consisting only of linear tentorial pits, parallel to the posterior edge of clypeus (Fig. 5a; *ftp*). Clypeus rectangular, ca. four times as wide as long, partially covering mandibles in dorsal view; dorsally with six stout setae placed lengthwise anteriorly and many short thin setae. Labrum (Fig. 5b) subtrapezoidal, dorsally with 8 long stout setae aimed anteriorly. Labral apex (Fig. 8e) double-arched, bearing two very short setae on the anterior edge. Epipharynx (Fig. 5c) anteriorly covered with rows of bulbous processes and a pair of two large bulbous sensoria anteromedially (Figs. 5c and 8e; *bs*) and a pair of differently shaped sensoria placed laterally. Pharynx covered with rows of setae and spines which project up to posterior edge of clypeus, with oblique transverse cibarial plates (Fig. 5c; *cp*) in labral-clypeal membrane area and a pair of sensoria placed posteromedially behind these plates. Ventral mouthparts retracted, forming a maxillo-labial complex (Fig. 8a). Hypostomal rods absent. Ventral epicranial ridges roughly reaching beyond the level of the posterior edge of the maxillo-labial complex. Gular region short with gular sutures converging anteriorly. Tentorium (Fig. 6) consisting of a pair of sclerotized anterior arms, hyaline dorsal arms and sclerotized posterior arms connected with posterior tentorial bridge. A pair of short sclerotized arms connected with filamentous secondary bridge growing dorsally from the middle of posterior arms. *Instar II* (Fig. 4 (b, e, h)). HW 1.484 ± 0.082 mm; HL 1.073 ± 0.082 mm; HW/HL 1.391 ± 0.145; length of gena about one third of the width of the head capsule in its longest width in dorsal view. Head capsule dorsally covered with long and several short stout setae. Epicranial suture and epicranial stem of light coloration. *Instar I* (Figs. 4 (c, f, i) and 5a, d). HW 1.108 ± 0.049 mm; HL 0.836 ± 0.103 mm; HW/HL 1.34 ± 0.139 times wider than long; length of gena about half of the width of the head capsule in its longest width in dorsal view.

Antennae (Fig. 7a–c): *Instar III.* Trimerous, inserted on lateral distal margin of gena; inserted in membranous socket. All antennomeres fully sclerotized and of similar length (AI 0.403 ± 0.034 mm, AII 0.414 ± 0.04 mm, AIII 0.353 ± 0.039 mm). Antennomere I cylindrical, slightly wider on distal end, sloping laterally towards the longitudinal axis of the larva, bearing no setae. Antennomere II club shaped, wider on distal end, sloping laterally towards the longitudinal axis of the larva bearing several stout setae unequally and scarcely scattered across the surface. Sensorium of antennomere II (Fig. 7c) placed on inner lateral area of its distal end together with three small but bulky sensilla lacking a socket, the longest one and the shortest one growing from the same base. Sensorium egg-shaped, widest at the base, encircled by a sclerotized ring, closely annealing to the second antennomere. Antennomere III placed on outer lateral area of antennomere II, bearing several stout setae mainly on its distal half (Fig. 7b). *Instar II.* All antennomeres fully sclerotized and of similar length (AI 0.294 ± 0.030 mm, AII 0.373 ± 0.022 mm, AIII

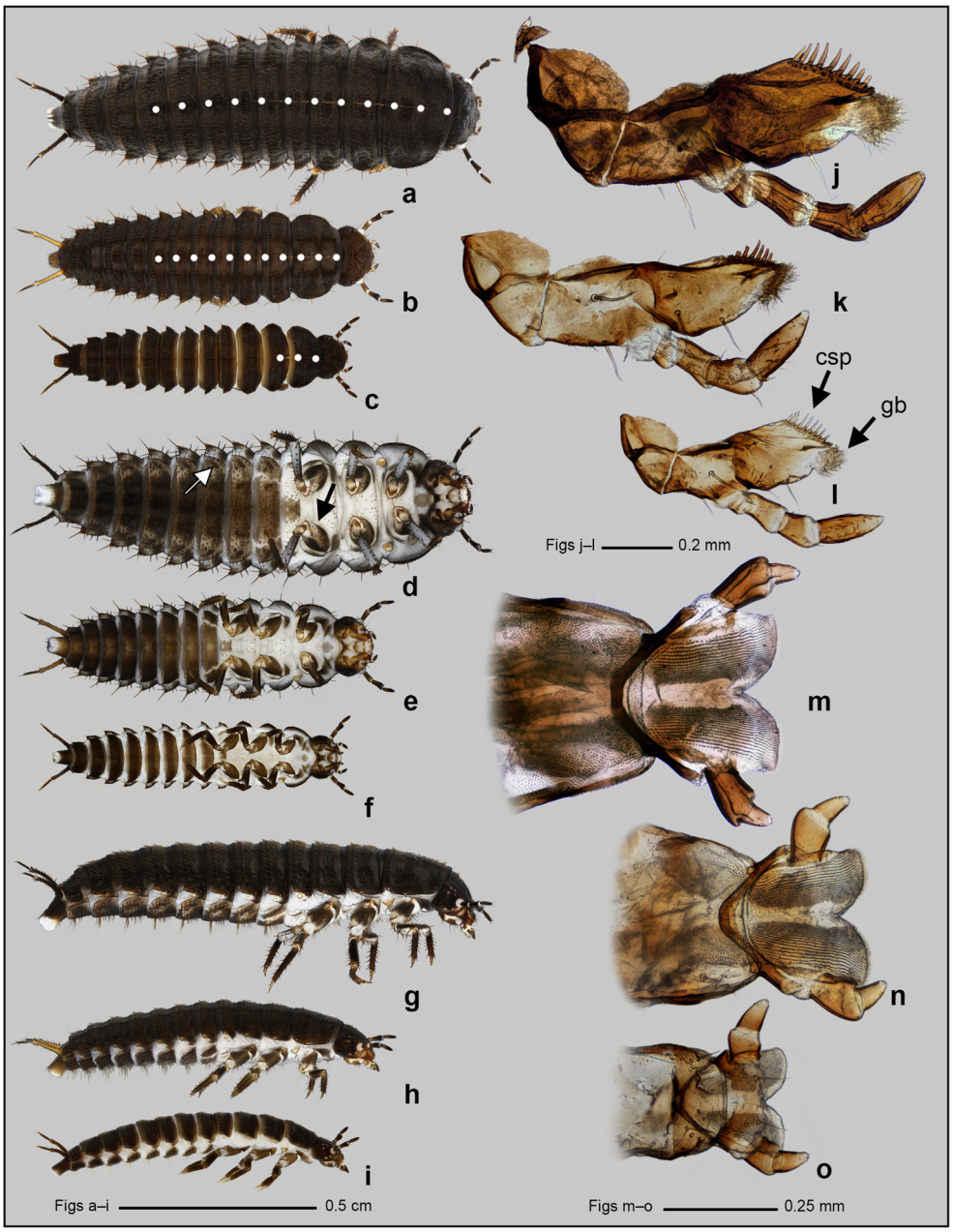

Fig. 4 *Thanatophilus rugosus*: dorsal habitus of third instar (a); second instar (b) and first instar (c) larva (sagittal line marked by white dots). Ventral habitus of third instar (d) (characteristic spots on abdominal ventrites (white arrow) and white inner side of coxa (black arrow)); second instar (e) and first instar (f) larva. Lateral view of third instar (g); second instar (h) and first instar (i) larva. Left maxilla of third instar (j); second instar (k) and first instar (l) larva. Labium of third instar (m); second instar (n) and first instar (o) larva. Abbreviations: csp—cuticular spines on lacinia; gb—brush of setae on galea

0.351 ± 0.015 mm). *Instar I.* All antennomeres fully sclerotized, antennomere I shortest (AI 0.213 ± 0.009 mm), antennomere II and III of similar length (AII 0.287 ± 0.025 mm, AIII 0.313 ± 0.016 mm).

Maxilla (Figs. 4 (j–l) and 8a): *Instar III* (Fig. 4j). Consisting of five parts (cardo, stipes, palpus, lacinia, and galea), attached to labium forming a maxillo-labial complex. Maxillary articulating areas present, completely unsclerotized. Lacinia and galea partly fused together. Cardo transverse, sub-triangular, ca. two times wider than long, with one short seta ventrolaterally close to the base of stipes. Stipes sub-rectangular, longer than wide, ventrally bearing one long stout seta in the center, one long stout seta outer-laterally and several short setae. Galea fixed, bearing two long setae outer-laterally, with a brush of very dense setation on its apex (Figs. 4 (l) and 8d; *gb*). Lacinia fixed, bearing 8 to 10 visible stout spines on its outer lateral margin (Fig. 4 (l); *csp*) together with an apical lobe bearing a short cuticular projection composed of several shorter spines grown together. Palpifer very short, sclerotized mainly on outer lateral margin. Maxillary palpus trimerous, palpomere I (Fig. 8a; *mpI*) cylindrical (MPI 0.201 ± 0.026 mm), ca. two times longer than wide; palpomere II (Fig. 8a; *mpII*) cylindrical (MPII 0.209 ± 0.011 mm), sloping laterally towards the longitudinal axis of the larva, palpomere III (Fig. 8a; *mpIII*) conical (MPIII 0.32 ± 0.033 mm), longest of the palpomeres. Palpifer and palpomeres sparsely covered by setae, palpomere III

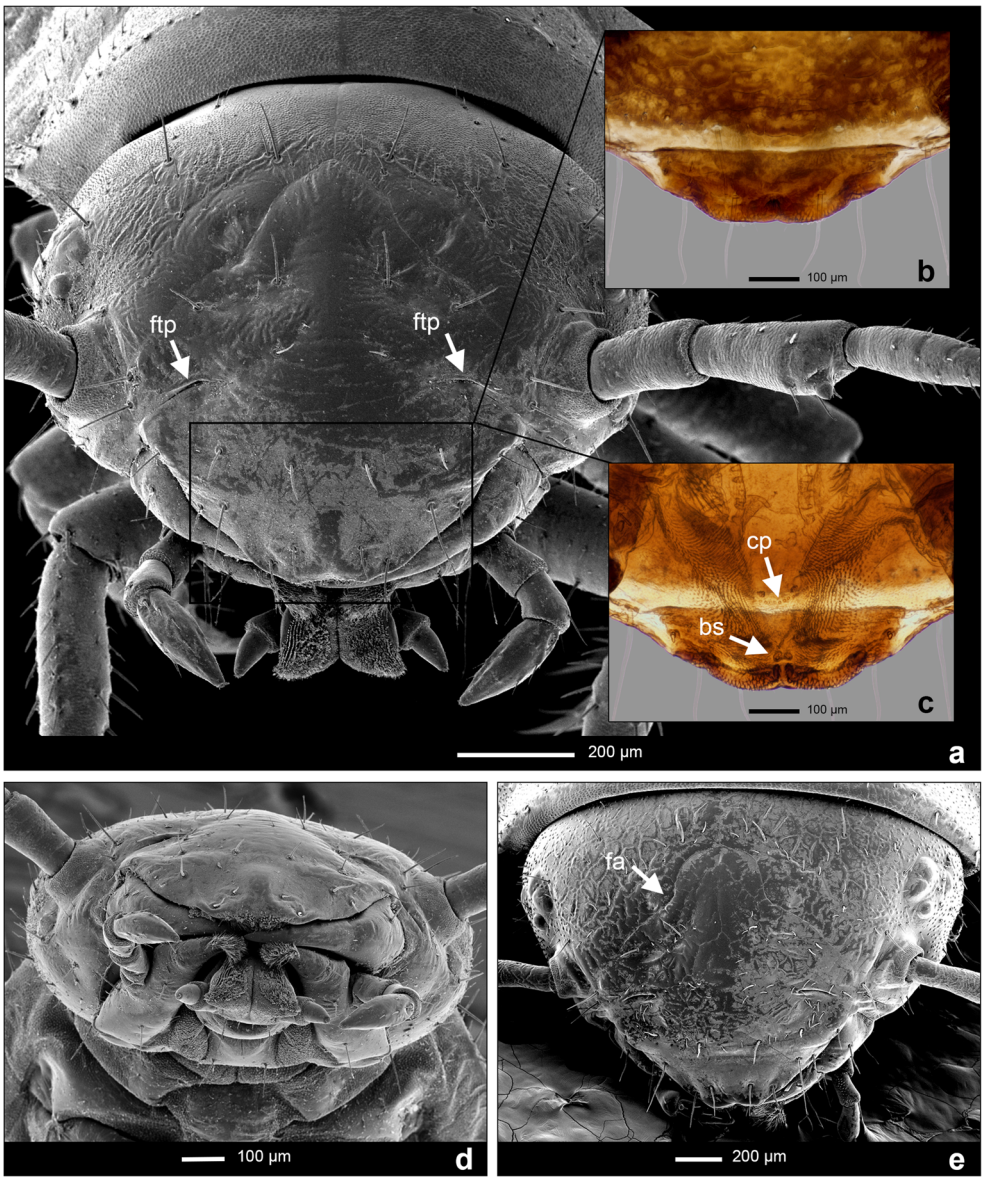

Fig. 5 *Thanatophilus rugosus*: head of first instar larva in dorsal view (**a**); detail of labrum of third instar larva in dorsal (**b**) and ventral (**c**) view. Head of first instar larva in frontal view (**d**); head of third instar larva in dorsal view (**e**). Abbreviations: bs—bulbous sensorium on epipharynx; cp—cibarial plates on pharynx; fa—frontal arm; ftp—frontal tentorial pit

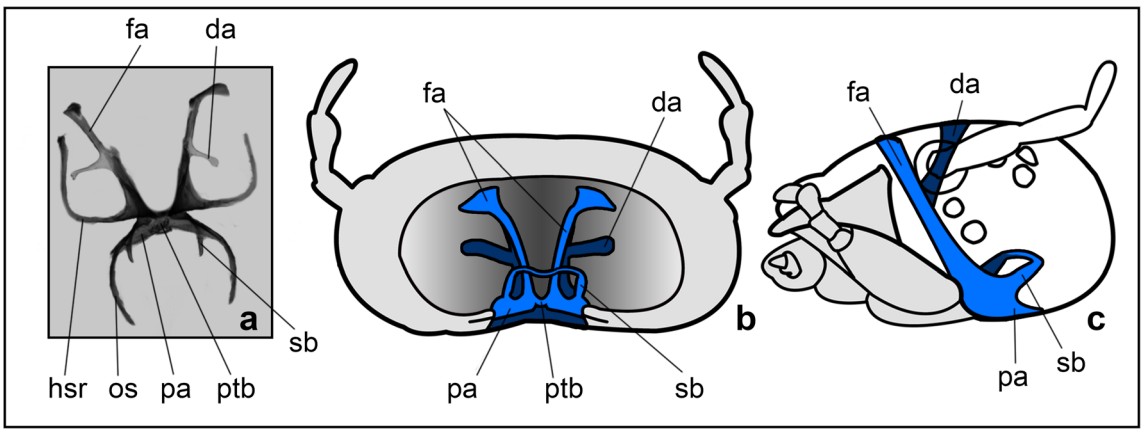

Fig. 6 *Thanatophilus rugosus*: tentorium in dorsal (**a**); posterior (**b**) and lateral (**c**) view. Abbreviations: da—dorsal arm; fa—frontal arm; hsr—hypostomal ridge; os—occipital suture; pa—posterior arm; ptb—posterior bridge; sb—short sclerotized arms connected with filamentous secondary bridge growing dorsally from the middle of posterior arms

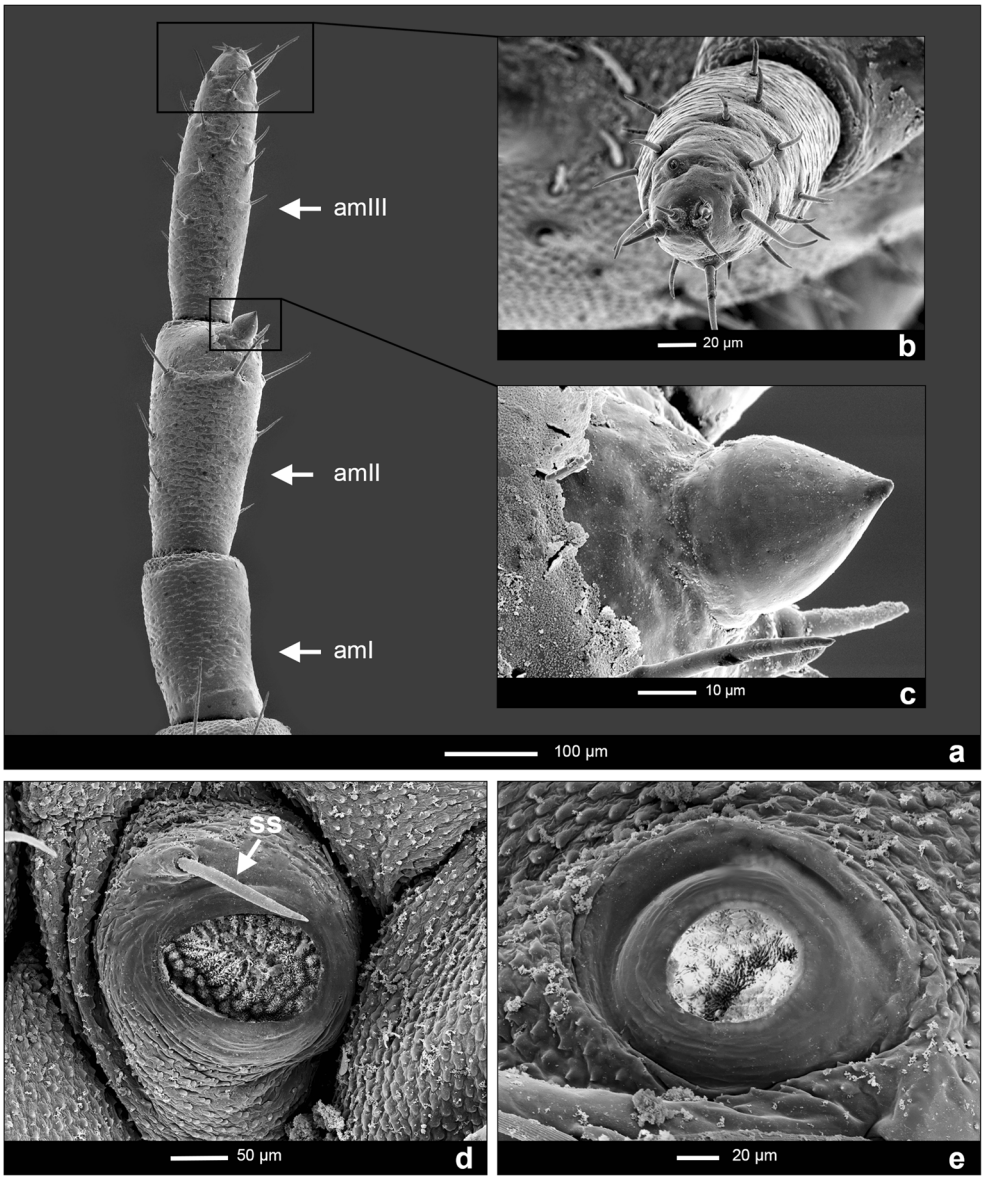

Fig. 7 *Thanatophilus rugosus*: left antenna of first instar larva in dorsal view (**a**); detail of third antennomere in frontal view (**b**); detail of antennal sensorium (**c**). Metathoracic (**d**) and abdominal (**e**) spiracle. Abbreviations: amI—antennomere I; amII—antennomere II; amIII—antennomere III; ss—seta on metathoracic spiracle

having a short stout seta in an articulated protuberance placed on outer-lateral edge of its base. The apex of palpomere III covered by short blunt peg-like sensilla (Fig. 8b). *Instar II* (Fig. 4 (k)). Palpomere lengths: MPI 0.146 ± 0.009 mm; MPII 0.133 ± 0.012 mm; MPIII 0.226 ± 0.021 mm. *Instar I* (Fig. 4 (l) and 8a). Palpomere lengths: 0.105 ± 0.01 mm; MPII 0.1 ± 0.011 mm; MPIII 0.181 ± 0.024 mm.

Labium (Figs. 4 (m–o) and 8a): *Instar III* (Fig. 4 (m)). Formed by prementum, mentum and submentum, all sclerotized on their basal areas (Fig. 8a; *pm*, *m*, *sm*). Ligula bi-lobed (Fig. 8a, d; *lig*); each lobe along the sagittal plane covered dorsally by a group of numerous longitudinal lines of fine short setation and dense bulbous projections apically and centrally between the two groups; ventrally, a pair of long setae is present in the lateral parts of the central area of prementum, as well as a pair of shorter setae in the basal half. Labial palpus bimerous (LPI 0.156 ± 0.014 mm, LPII 0.083 ± 0.007 mm), with no setation; basal palpomere (Fig. 8a; *lpI*) club-shaped, sloping laterally towards the longitudinal axis of the larva, distal palpomere (Fig. 8a; *lpII*) conical, blunt, ca. one third of the length of basal palpomere, bearing a group of short blunt peg-like sensilla on its apex (Fig. 8c). Mentum longer than wide, sub-oval, with dark pigmentation on its base; ventrally bearing two pairs of long setae on its posterior half. Submentum bearing a pair of long stout and several shorter thin setae, paired or irregularly scattered posterolaterally, alongside its sclerotized distal half when viewed ventrally. *Instar II* (Fig. 4 (n)). Labial palpi lengths: LPI 0.109 ± 0.009 mm, LPII 0.072 ± 0.008 mm. *Instar I* (Fig. 4 (o)). Labial palpi lengths: LPI 0.080 ± 0.006 mm, LPII 0.083 ± 0.01 mm.

Mandibles (Fig. 9a, b, f–i): *Instar III* (Fig. 9a, b). Symmetrical, simple without mola or prostheca, basal half

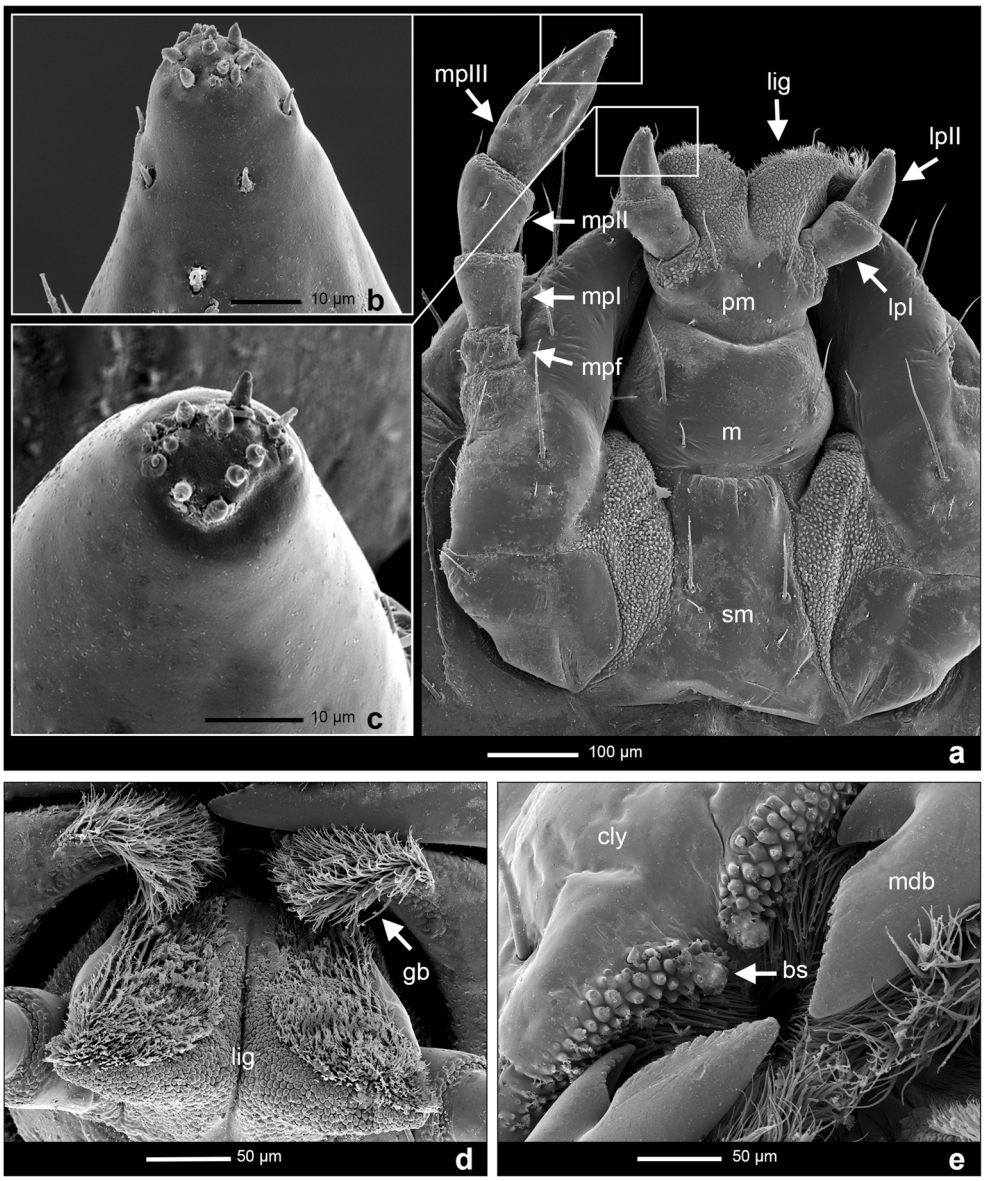

Fig. 8 *Thanatophilus rugosus*: maxillo-labial complex of first instar larva in ventral view (**a**); detail of apices of labial palpomere II (**b**) and maxillary palpomere III (**c**). Detail of ligula (**d**) and labrum (**e**) in frontal view. Abbreviations: bs—bulbous sensorium on epipharynx; gb—brush of setae on galea; lig—ligula; lpI—labial palpomere I; lpII—labial palpomere II; m—mentum; mdb—mandible; mpI—maxillary palpomere I; mpII—maxillary palpomere II; mpIII—maxillary palpomere III; mpf—maxillary palpifer; pm—prementum; sm—submentum

consisting of wide triangular base in dorsoventral cross section, distal half more dorsoventrally flattened, apex consisting of two scissorial teeth lying obliquely, perpendicular to the plane of movement of the mandible, apical tooth (Fig. 9g; *at*) longer and serrated laterointernally, sub-apical tooth (Fig. 9g–i; *st*) shorter, positioned dorsally towards the outer tooth and serrated lateroexternally towards the serrated area of the outer tooth. One long stout seta present laterodorsally on mandibular base (Fig. 5d) and one short stout seta present outerlaterally in the mid-length of the mandible (Fig. 9f; *ms*). Left mandible larger, covering the apex of the right mandible when clenched (Fig. 5d). *Instar II* (Fig. 9f, g). Same as Instar III. *Instar I*. Same as Instar III.

Thorax (Fig. 4 (a–i)): *Instar III* (Fig. 4 (a, d, g)). Three-segmented, thoracic tergites divided by sagittal line; paraterga slightly overlapping the body forming irregular semicircles. Pronotum (N1W 3.054 ± 0.377 mm, N1L 1.186 ± 0.154 mm) sub-oval, wider posteriorly, rounded at posterolateral corners. Mesonotum (N2W 3.413 ± 0.511 mm; N2L 0.698 ± 0.106 mm) and metanotum (N3W 3.515 ± 0.459 mm; N3L 0.631 ± 0.068 mm) sub-oval, similar in shape and size. Ventrolateral areas of prothorax, mesothorax, and metathorax formed by sclerotized episternum and epimeron; spiracular sclerite of mesothorax mostly membranous (except for inner anterior edge), bearing a large (relative to abdominal spiracles) annular spiracle (Figs. 4 (d, g) and 7d) with yellow-colored peritreme and bearing one long stout seta on its inner lateral margin. The atrium (inner chamber) padded with shrub-like filtration hairs. Presternum short, semi-lens shaped, wider than long, subdivided into three plates; lateral ones well sub-triangular, well sclerotized; medial plate sub-rectangular, semi-sclerotized, reaching edges of the presternum both anteriorly and

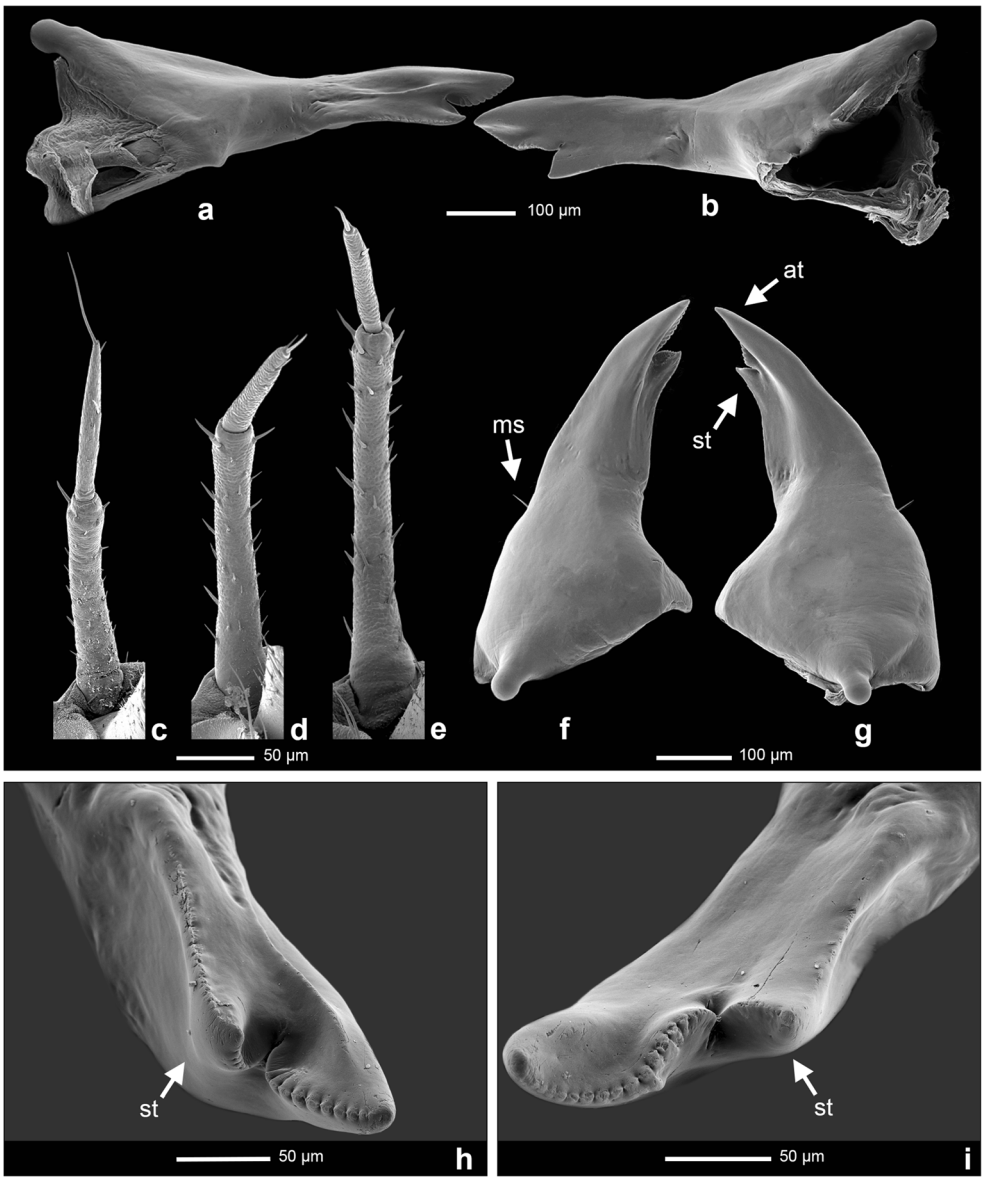

Fig. 9 *Thanatophilus rugosus*: left (**a**) and right (**b**) mandible of third instar larva in posterior view. Urogomphi of first (**c**), second (**d**), and third (**e**) instar larva. Left (**f**) and right (**g**) mandible of second instar larva in dorsal view. Detail of apices of left (**h**) and right (**i**) mandible of third instar larva in frontal-ventral view. Abbreviations: at—apical tooth; ms—seta present outer-laterally in the mid-length of the mandible; st—sub-apical tooth

posteriorly. Mesosternum and metasternum sub-divided by transverse fold into membranous basisternum and sternellum. *Instar II* (Fig. 4 (b, e, h)). Pronotum sub-oval (N1W 2.038 ± 0.193 mm; N1L 0.946 ± 0.089 mm), wider posteriorly, rounded at posterolateral corners. Mesonotum (N2W 2.26 ± 0.231 mm; N2L 0.474 ± 0.029 mm) and metanotum (N3W 2.363 ± 0.321 mm; N3L 0.398 ± 0.062 mm) sub-oval, similar in shape and size. Presternum medial plate sub-rectangular, poorly sclerotized, reaching only posterior edge of the presternum. *Instar I* (Fig. 4 (c, f, i)). Pronotum (N1W 1.476 ± 0.064 mm; N1L 0.622 ± 0.08 mm) semicircular, wider posteriorly, rounded at posterolateral corners. Mesonotum (N2W 1.595 ± 0.077 mm; N2L 0.303 ± 0.024 mm) and metanotum sub-oval, similar in shape and size. Metanotum (N3W 1.655 ± 0.094 mm; N3L 0.261 ± 0.015 mm). Presternal medial plate sub-circular, not reaching posterior nor anterior edge of the presternum.

Abdomen (Fig. 4 (a–i)): *Instar III* (Fig. 4 (a, d, g)). Ten-segmented, tapering posteriad, segments I to IV dorsally sub-divided by fine sagittal line anteriorly (Fig. 4 (a)), on segment IV barely visible. Tergites of segments I to VIII sub-rectangular, narrow, A1W 3.384 ± 0.473 mm; A1L 0.454 ± 0.072 mm, similar in shape and coloration, with posteriorly pointed paratergites. Tergite of segment IX sub-rectangular, bearing paired, well-developed two-segment urogomphi (Fig. 9e) that are inserted dorsolaterally. Basal segment of urogomphi narrow (URI 1.078 ± 0.118 mm), wider on proximal and distal ends, slightly bent posteromedially, bearing short stout setae; distal segment slender (URII 0.49 ± 0.051 mm), cylindrical, with one seta inserted on the apex (URS 0.117 ± 0.012 mm) and two setae inserted slightly below the apex; first dorsally and second inner-ventrolaterally. Segment X dorsally sub-trapezoidal, forming a well-sclerotized cylinder; distal central

half of dorsal area with two longitudinal lines of white pigmentation; segment X holding the hold-fast organ (pygopod) with several eversible processes. Ventrites of segments I to VIII sub-trapezoidal; ventrite of segment IX sub-rectangular. Spiracles (Figs. 4 (d) and 7e) annular, with yellow-colored peritreme and bearing no setae. Spiracle on segment I is the largest of abdominal spiracles. *Instar II* (Fig. 4 (b, e, h)). Tergites of segments I to VIII sub-rectangular, narrow, A1W 2.351 ± 0.293 mm; A1L 0.279 ± 0.043 mm, similar in shape and coloration. Basal segment of urogomphi (Fig. 9d) narrow (URI 0.8 ± 0.040 mm), distal segment slender (URII 0.442 ± 0.039 mm), cylindrical, ca. half as long as basal segment, with one seta inserted on the apex (URS 0.131 ± 0.2 mm). *Instar I* (Fig. 4 (c, f, i)). Tergites of segments I to VIII sub-rectangular, A1W 1.568 ± 0.108 mm, A1L 0.184 ± 0.015 mm, basal segment of urogomphi (Fig. 9c) narrow, URI 0.554 ± 0.035 mm, distal segment slightly slender and cylindrical, but almost the same length URII 0.449 ± 0.043 mm, with long terminal seta (URS 0.207 ± 0.066 mm).

Legs (Figs. 4 (d–f) and 10a–d): *Instar III* (Figs. 4 (a) and 10a). Pentamerous including pretarsus, all pairs similar in shape and size. Coxa large, stout, covered by stout setae; with white pigmentation on the posterior and anterior area of the apex; coxal-trochanteal membrane reaching ca. one third of longitudinal length. Trochanter small, sub-triangular in lateral view, centrally white pigmented and sclerotized only basally and distally, covered by several stout setae of the same length as coxa and one seta ca. three to four times longer than the rest, placed ventrally on the distal end. Femur cylindrical, dorsally sclerotized. Ventrally completely white, bearing two longitudinal lines of sharp stout setae (number of setae in these lines vary from 5 to 10 and no systematic difference was revealed)

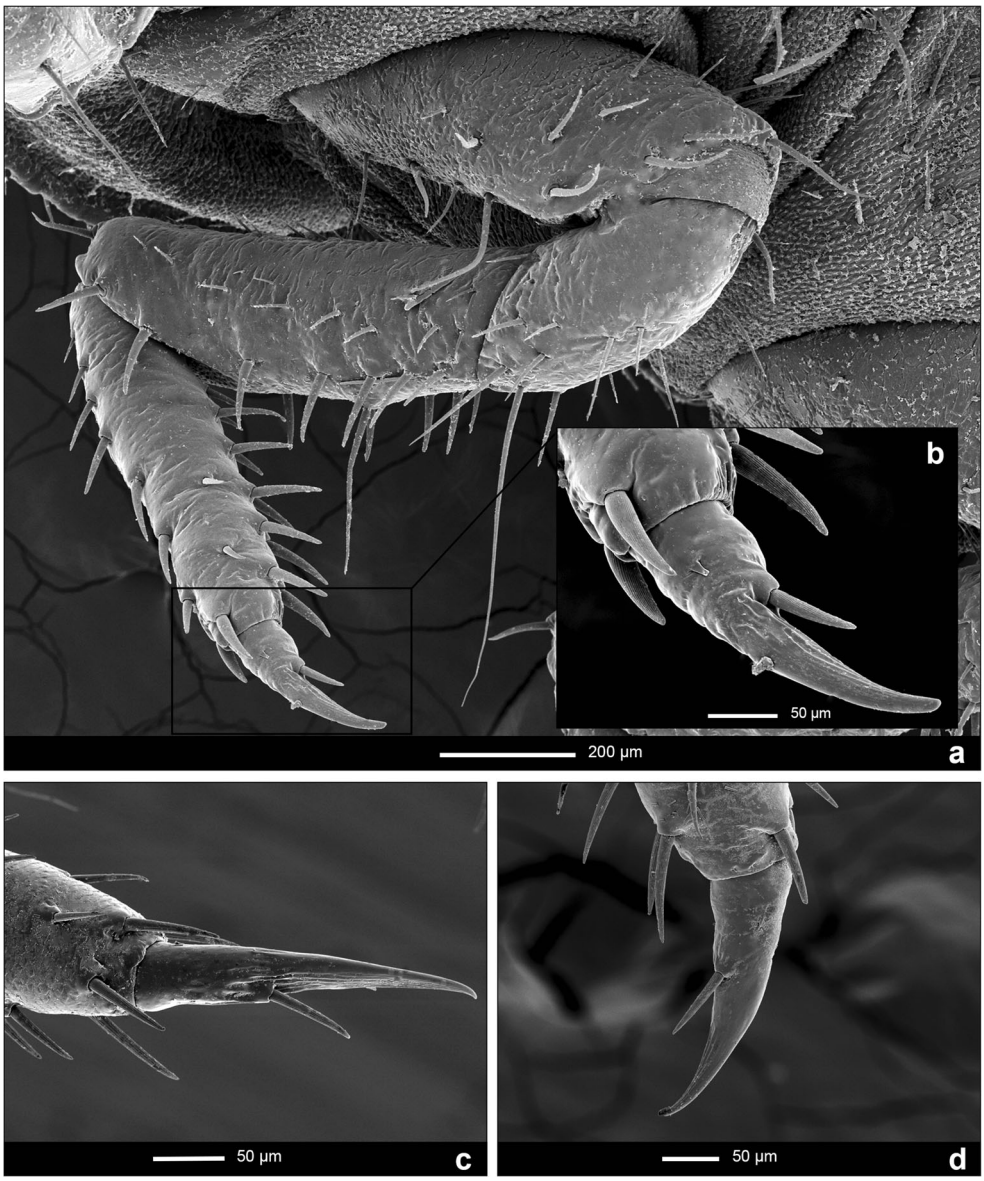

Fig. 10 *Thanatophilus rugosus*: leg of third instar larva in lateral view (**a**). Detail of tarsal claw of third instar (**b**); first instar (**c**) and second instar (**d**) larva

and a very long seta (ca. two times the length of neighboring setae) between these lines; several other irregular longitudinal lines with shorter setation placed laterally and dorsally. Tibiotarsus ca. as long as femur, narrower, tapering towards distal end, bearing several longitudinal lines of stout sharp setae around its circumference followed by less regular lines of shorter setae. Pretarsus (Fig. 10b) composed of a claw with bulky base, ventrally bearing one stout seta of ca. one third of the length of pretarsus, placed in the mid-length of the claw. Common setae on coxa and trochanter generally thinner and slightly longer than stout strong setae on femur and tibiotarsus. *Instar II* (Fig. 4 (e)). Trochanter small, sub-triangular in lateral view, centrally white pigmented and darker only proximal and distal ends. Femur cylindrical, fully sclerotized and dark pigmented, bearing two longitudinal lines of sharp stout setae ventrally with one ca. two to three times longer seta centrally between the two lines. Claw (Fig. 10d) appears to be more slender than in instar III. *Instar I* (Fig. 4 (f)). Trochanter small, sub-triangular in lateral view, dark pigmented with weak lighter patch on the central area. Claw (Fig. 10c) more slender than in later instars, with narrow base.

Pupa (Fig. 11)

Type of pupa: *adectica exarata libera*. Curved, ventrally concave. Length 9.3 mm. Coloration: cream white body with dark-brown setae.

Head capsule: partially covered by pronotum in dorsal view. Antennae short, extending laterally, without reaching posterolateral corners of pronotum. Mouthparts visible in ventral view.

Thorax: surface of pronotum covered by numerous short brown hairs, with two pairs of long stout dark-brown setae on its anterolateral edge (Fig. 11b; *ps*). Pronotum similar in shape to that of adult by wavy cutting of its posterior margin, but less convex anteriorly. Mesonotum shorter but wider than metanotum, with distinct triangular protuberance posteromedially representing future scutellum of adult. Wing pads and rectangular elytra completely white and about the same length; wing pads reaching fourth abdominal segment. Prothoracic and mesothoracic legs free, visible in ventral view; tibiae of metathoracic legs partially covered by wing pads, distal segments of tarsi extend to seventh abdominal segment. Spiracles present on pleural areas of mesothorax.

Abdomen: abdominal segments sub-rectangular, wider than long. Segments II–VII bearing pairs of long stout dark-brown setae (Fig. 11a; *as*). Urogomphi on segment VIII short and bulky, white, with dark-brown apices bearing medium-long stout dark-brown setae (Fig. 11b, c; *us*). Spiracles present on abdominal pleural areas of segments I–VIII, on segments I–IV light-brown, otherwise white.

Differential diagnose of larval instars

Instar I. Body length 5.96 ± 0.868 mm, head width 1.108 ± 0.49 mm. Basal segment of urogomphi almost as long as the second one and terminal seta half of the length of the second

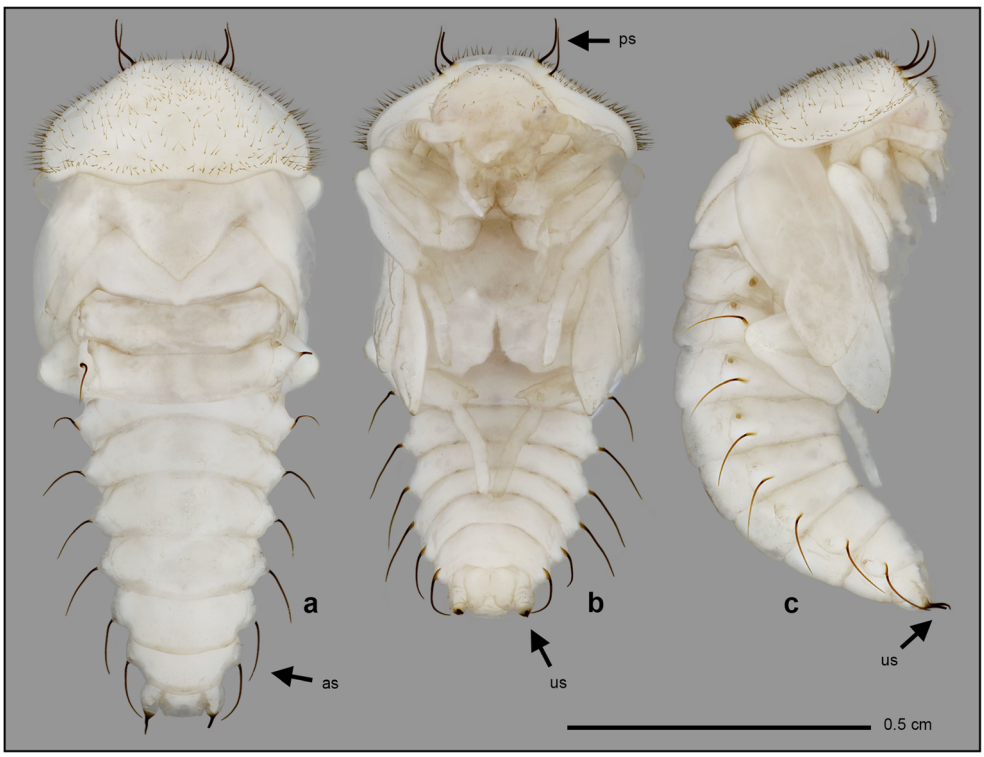

Fig. 11 *Thanatophilus rugosus*: pupa in dorsal (**a**), ventral (**b**) and lateral (**c**) view. Abbreviations: as—abdominal setae; ps—pronotal setae; us—urogomphal setae

segment (Fig. 9c). Abdominal ventrites 2–9 uniformly brown (Fig. 4 (f)). Sagittal line terminated on metathorax (Fig. 4 (c)). Inner side of all coxa brown (Fig. 4 (f)).

Instar II. Body length 9.22 ± 1.450 mm, head width 1.484 ± 0.082 mm. Basal segment of urogomphi approximately twice the length of the second segment and terminal seta less than one third of the length of the second segment (Fig. 9d). Abdominal ventrites 2–9 uniformly brown with slight discoloration in the middle (Fig. 4 (e)). Sagittal line terminated on the abdominal segment III or IV (Fig. 4 (b)). Inner side of all coxa brown (Fig. 8).

Instar III. Body length 13.25 ± 1.488 mm, head width 1.953 ± 0.15 mm. Basal segment of urogomphi approximately twice the length of the second segment and terminal seta less than one third of the length of the second segment (Fig. 9e). Abdominal ventrites 2–8 light brown with dark brown spots on the lateral edges and darker more uniform line in the middle (Fig. 4 (d)). Sagittal line terminated on abdominal segment V or VI (Fig. 4 (a)). Inner side of all coxa white (Fig. 4 (d)).

Discussion

Previous descriptions of developmental stages of *T. rugosus* by Xambeu [38] and von Lengerken [33] were rather brief (not including some important morphological features like labium, maxillae, nor tentorium), and most of the characters are only mentioned in the text form without accessory images. Von Lengerken [33] attempted to include a description of differences among larval instars of all three species of the genus *Thanatophilus* (*T. dispar*, *T. rugosus*, and *T. sinuatus*) and offered several size-based characteristics. Nevertheless, he acknowledged that these values are highly variable and may not be reliable. According to our findings, some species characteristics like overall body shape or size of protergites recognized by von Lengerken [33] are highly variable among specimens and thus of limited use. Von Lengerken's description also did not mention differences in coloration between *T. rugosus* and *T. sinuatus* as their third instars can be very easily distinguished by white markings along the margins of the body of the latter.

Head width and other size-based characteristics with accompanying statistical models are often suggested as a means to easily identify larval instars of necrophagous beetles [17–21]. This approach is very popular thanks to its accessibility, but the accuracy of the results is doubtful [33]. Although we did not find an overlap among head widths of all three examined larval instars, we agree with the idea that geographical region, temperature, quality, and abundance of food and other variables can have a profound effect on larval size [22, 33]. Qualitative characters like proportions of body parts, cheatotaxy, coloration, and other traits not affected by the size of the individual seem to be more reliable, and their utilization minimizes the probability of error.

One of the reasons of quantitative characters for instar identification being developed for forensically important beetle species is the belief that majority of their larvae lack qualitative identifying characters [19]. Kilian and Madra [48] challenged this idea by finding several qualitative characters for instar identification of *Sciodrepoides watsoni* (Spence, 1813) (Coleoptera: Leiodidae: Cholevinae). Our results also contradict the idea and we reckon that future morphological re-descriptions of larvae will prove us right. We found several uncommon characters that could be used for instar determination such as differences in appearance of claws, length of sagittal line, or relative position of presternal medial plate.

The difference in appearance of claws is very slight, nonetheless possibly applicable to other species as well. We believe it is worth mentioning additional to other more obvious differences. The length of the sagittal line seems to be closely related to individual development and can be observed even on the larval exuvia. Our unpublished data suggest that this character could be applicable also to other species of the genus *Thanatophilus*.

One of the less obvious and more challenging characters to use for instar identification could be the relative position of the presternal medial plate, which differs among instars. In the first instar, it does not reach up to the anterior or posterior edge while in other two instars it reaches either the posterior edge (Instar II) or both edges (Instar III). This character is rather crude as the presternal median plate is flexible and may not be fully visible in some individuals, thus we did not include it into the differential diagnose of larval instars. Nonetheless, it is worth mentioning.

Our article provides detailed morphological re-description of all larval instars of *T. rugosus*. This will allow identification of the species and all its instars regardless of their size or stage of development. The results can be further used in basic and applied fields of science such as developmental biology and forensic entomology.

Acknowledgements Thanks are due to Miroslav Hyliš (Praha, Czech Republic) for preparing our electron imaging samples and providing needed guidance at the SEM laboratory.

Funding information The project was supported by the Ministry of the Interior of the Czech Republic (grant no. VI20152018027).

Compliance with ethical standards

Conflict of interest H. Šuláková is an employee of the Faculty of Environmental Sciences and Police of the Czech Republic.

Ethical approval All applicable international, national, and/or institutional guidelines for the care and use of animals were followed.

References

1. Midgley JM, Richards CS, Villet MH (2010) The utility of Coleoptera in forensic investigations. In: Amendt J, Goff ML, Campobasso CP, Grassberger M (eds) Curr. Concepts Forensic Entomol. Springer Netherlands, Dordrecht, pp 57–68
2. Midgley JM, Villet MH (2009) Development of *Thanatophilus micans* (Fabricius 1794) (Coleoptera: Silphidae) at constant temperatures. Int J Legal Med 123(4):285–292. https://doi.org/10.1007/s00414-008-0280-0
3. Bourel B, Tournel G, Hédouin V, Lee Goff ML, Gosset D (2001) Determination of drug levels in two species of necrophagous Coleoptera reared on substrates containing morphine. J Forensic Sci 46(3):600–603. https://doi.org/10.1520/JFS15010J
4. Matuszewski S, Szafałowicz M, Jarmusz M (2013) Insects colonising carcasses in open and forest habitats of Central Europe: search for indicators of corpse relocation. Forensic Sci Int 231(1-3): 234–239. https://doi.org/10.1016/j.forsciint.2013.05.018
5. Ridgeway JA, Midgley JM, Collett IJ, Villet MH (2014) Advantages of using development models of the carrion beetles *Thanatophilus micans* (Fabricius) and *T. mutilatus* (Castelneau) (Coleoptera: Silphidae) for estimating minimum post mortem intervals, verified with case data. Int J Legal Med 128(1):207–220. https://doi.org/10.1007/s00414-013-0865-0
6. Charabidze D, Vincent B, Pasquerault T, Hedouin V (2016) The biology and ecology of *Necrodes littoralis*, a species of forensic interest in Europe. Int J Legal Med 130(1):273–280. https://doi.org/10.1007/s00414-015-1253-8
7. Goff LM (2010) Early postmortem changes and stages of decomposition. In: Amendt J, Goff ML, Campobasso CP, Grssberger M (eds) Curr. Concepts Forensic Entomol. Springer, Dordrecht, pp 1–24
8. Rivers D, Dahlem G (2014) The science of forensic entomology. John Wiley & Sons, Inc., Chichester
9. Richards CS, Villet MH (2008) Factors affecting accuracy and precision of thermal summation models of insect development used to estimate post-mortem intervals. Int J Legal Med 122(5):401–408. https://doi.org/10.1007/s00414-008-0243-5
10. Amendt J, Krettek R, Zehner R (2004) Forensic entomology. Naturwissenschaften 91(2):51–65. https://doi.org/10.1007/s00114-003-0493-5
11. Wells JD, Sperling FAH (2001) DNA-based identification of forensically important Chrysomyinae (Diptera: Calliphoridae). Forensic Sci Int 120(1-2):110–115. https://doi.org/10.1016/S0379-0738(01)00414-5
12. Wells JD, Pape T, Sperling FAH (2001) DNA-based identification and molecular systematics of forensically important Sarcophagidae (Diptera). J Forensic Sci 45(5):1098–1102. https://doi.org/10.1520/JFS15105J
13. Willows-Munro S, Schoeman MC (2015) Influence of killing method on Lepidoptera DNA barcode recovery. Mol Ecol Resour 15(3): 613–618. https://doi.org/10.1111/1755-0998.12331
14. Cho S, Epstein SW, Mitter K, Hamilton CA, Plotkin D, Mitter C, Kawahara AY (2016) Preserving and vouchering butterflies and moths for large-scale museum-based molecular research. Peer J 4: e2160. https://doi.org/10.7717/peerj.2160
15. Dyar HG (1890) The number of molts of Lepidopterous larvae. Psyche A J Entomol 5:420–422
16. Klingenberg CP, Zimmermann M (1992) Dyar rule and multivariate allometric growth in 9 species of waterstriders (Heteroptera, Gerridae). J Zool 227(3):453–464. https://doi.org/10.1111/j.1469-7998.1992.tb04406.x
17. Midgley JM, Villet MH (2009) Effect of the killing method on post-mortem change in length of larvae of *Thanatophilus micans* (Fabricius 1794) (Coleoptera: Silphidae) stored in 70% ethanol. Int J Legal Med 123(2):103–108. https://doi.org/10.1007/s00414-008-0260-4
18. Velásquez Y, Viloria AL (2010) Instar determination of the neotropical beetle *Oxelytrum discicolle* (Coleoptera: Silphidae). J Med Entomol 47(5):723–726. https://doi.org/10.1603/me09058
19. Fratczak K, Matuszewski S (2014) Instar determination in forensically useful beetles *Necrodes littoralis* (Silphidae) and *Creophilus maxillosus* (Staphylinidae). Forensic Sci Int 241:20–26. https://doi.org/10.1016/j.forsciint.2014.04.026
20. Frątczak K, Matuszewski S (2016) Classification of forensically-relevant larvae according to instar in a closely related species of carrion beetles (Coleoptera: Silphidae: Silphinae). Forensic Sci Med Pathol 12(2):193–197. https://doi.org/10.1007/s12024-016-9774-0
21. Jakubec P (2016) Thermal summation model and instar determination of all developmental stages of necrophagous beetle, *Sciodrepoides watsoni* (Spence) (Coleoptera: Leiodidae: Cholevinae). Peer J 4:e1944. https://doi.org/10.7717/peerj.1944
22. Stillwell RC, Fox CW (2009) Geographic variation in body size, sexual size dimorphism and fitness components of a seed beetle: local adaptation versus phenotypic plasticity. Oikos 118(5):703–712. https://doi.org/10.1111/j.1600-0706.2008.17327.x
23. Anderson RS, Peck SB (1985) The insects and arachnids of Canada, part 13: the carrion beetles of Canada and Alaska (Coleoptera: Silphidae and Agyrtidae). Agriculture Canada, Ottawa
24. Navarette-Heredia JL (2009) Silphidae (Coleoptera) de México: diversidad y distribución. Universidad de Guadalajara, Guadalajara
25. Růžička J (2015) Silphidae. In: Löbl I, Löbl D (eds) Cat. Palaearct. Coleopt. Vol. 2/1. Hydrophiloidea–Staphylinoidea, Revis. Updat. Ed. Brill, Leiden & Boston, pp 291–304
26. Dobler S, Müller JK (2000) Resolving phylogeny at the family level by mitochondrial cytochrome oxidase sequences: phylogeny of carrion beetles (Coleoptera, Silphidae). Mol Phylogenet Evol 15: 390–402. https://doi.org/10.1006/mpev.1999.0765
27. Sikes DS, Trumbo ST, Peck SB (2005) Silphinae. In: Tree Life Web Proj. http://tolweb.org/Silphinae/26994/2005.02.07. Accessed 26 Jul 2017
28. Schawaller W (1981) Taxonomie und Faunistik der Gattung *Thanatophilus* (Coleoptera: Silphidae). Stuttg Beitr Naturkunde, Ser A 351:1–21
29. Kozminykh VO (1994) A new species of carrion beetles of the genus *Thanatophilus* (Coleoptera, Silphidae) from the southern Urals. Zool Zhurnal 73:161–165
30. Růžička J (2002) Taxonomic and nomenclatorial notes on Palaearctic Silphinae (Coleoptera : Silphidae). Acta Soc Zool Bohemicae 66:303–320
31. Ji Y (2012) The carrion beetles of China (Coleoptera: Silphidae). China Forestry Publishing House, Beijing
32. Daniel CA, Midgley JM, Villet MH (2017) Determination of species and instars of the larvae of the afrotropical species of *Thanatophilus* Leach, 1817 (Coleoptera, Silphidae). African Invertebr 58(2):1–10. https://doi.org/10.3897/AfrInvertebr.58.12966
33. von Lengerken H (1929) Studien über die Lebenserscheinungen der Silphini (Col.). XI-XIII. *Thanatophilus sinuatus* F., *rugosus* L. und *dispar* Hrbst. Z Morphol Ökol Tiere 14:654–666
34. von Lengerken H (1938) Beziehungen zwischen der Ernährungsweise und der Gestaltung der Mandibeln bei den Larven der Silphini (Coleopt.) Zool Anz 122:171–175
35. Dorsey CK (1940) A comparative study of the larvae of six species of Silpha (Coleoptera, Silphidae). Ann Entomol Soc Am 33(1): 120–134. https://doi.org/10.1093/aesa/33.1.120
36. Paulian R (1941) Les premiers états des Staphylinoidea. Étude de morphologie comparée Mém Mus Natl Hist Nat (Nouv Ser) 15:1–361
37. Prins AJ (1984) Morphological and biological notes on some South African arthropods associated with decaying organic matter. Part 2.

The predatory families Carabidae, Hydrophilidae, Histeridae, Staphylinidae and Silphidae (Coleoptera). Ann South African Mus 92:295–365
38. Xambeu PJV (1900) Moeurs et métamorphoses d'insectes, 9e mémoire, deuxieme partie. Rev Entomol Caen 19:1–56
39. Xambeu PJV (1892) Moeurs et métamorphoses d'insectes (Suite). Ann Soc Linn Lyon 39:137–194
40. Anderson RS (1987) Scientific note. The larva of *Thanatophilus trituberculatus* (Kirby) (Coleoptera: Silphidae). Coleopt Bull 41:34
41. Kočárek P (2003) Decomposition and Coleoptera succession on exposed carrion of small mammal in Opava, the Czech Republic. Eur J Soil Biol 39(1):31–45. https://doi.org/10.1016/S1164-5563(02)00007-9
42. Matuszewski S, Bajerlein D, Konwerski S, Szpila K (2010) Insect succession and carrion decomposition in selected forests of Central Europe. Part 2: composition and residency patterns of carrion fauna. Forensic Sci Int 195(1-3):42–51. https://doi.org/10.1016/j.forsciint.2009.11.007
43. Dekeirsschieter J, Verheggen FJ, Haubruge E, Brostaux Y (2011) Carrion beetles visiting pig carcasses during early spring in urban, forest and agricultural biotopes of Western Europe. J Insect Sci 11:73. https://doi.org/10.1673/031.011.7301
44. Velásquez Y, Viloria AL (2009) Effects of temperature on the development of the Neotropical carrion beetle *Oxelytrum discicolle* (Brullé, 1840) (Coleoptera: Silphidae). Forensic Sci Int 185(1-3):107–109. https://doi.org/10.1016/j.forsciint.2008.12.020
45. Matuszewski S (2011) Estimating the pre-appearance interval from temperature in *Necrodes littoralis* L. (Coleoptera: Silphidae). Forensic Sci Int 212(1-3):180–188. https://doi.org/10.1016/j.forsciint.2011.06.010
46. Novák M (2017) Redescription of immature stages of central European fireflies, part 1: *Lampyris noctiluca* (Linnaeus, 1758) larva, pupa and notes on its biology (Coleoptera: Lampyridae: Lampyrinae). Zootaxa 4247:429–444. https://doi.org/10.11646/zootaxa.4247.4.5
47. Lawrence JF, Slipinski SA (2013) Australian beetles. Volume 1: morphology, classification and keys. CSIRO Publishing, Collingwood
48. Kilian A, Mądra A (2015) Comments on the biology of *Sciodrepoides watsoni watsoni* (Spence, 1813) with descriptions of larvae and pupa (Coleoptera: Leiodidae: Cholevinae). Zootaxa 3955(1):45–61. https://doi.org/10.11646/zootaxa.3955.1.2 10.11646/zootaxa.3955.1.2